

**TRIS (8-HYDROXYQUINOLINATE) METALS FOR  
SOLUTION-PROCESSED ORGANIC SOLAR CELLS**

**FAHMI FARIQ MUHAMMAD**

**THESIS SUBMITTED IN FULFILLMENT OF  
THE REQUIREMENT FOR THE DEGREE  
OF DOCTOR OF PHILOSOPHY**

**DEPARTMENT OF PHYSICS  
FACULTY OF SCIENCE  
UNIVERSITY OF MALAYA  
KUALA LUMPUR**

**2012**

# UNIVERSITI MALAYA

## ORIGINAL LITERARY WORK DECLARATION

Name of Candidate: **Fahmi Fariq Muhammad** (I.C/Passport No: **G2117848** )

Registration/Matric No: **SHC080054**

Name of Degree: **Doctor of Philosophy, PhD**

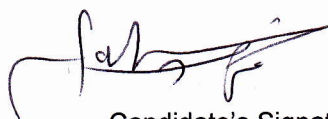
Title of Project Paper/Research Report/Dissertation/Thesis ("this Work"):

**TRIS (8-HYDROXYQUINOLINATE) METALS FOR SOLUTION-PROCESSED ORGANIC SOLAR CELLS**

Field of Study: **Solar Energy**

I do solemnly and sincerely declare that:

- (1) I am the sole author/writer of this Work;
- (2) This Work is original;
- (3) Any use of any work in which copyright exists was done by way of fair dealing and for permitted purposes and any excerpt or extract from, or reference to or reproduction of any copyright work has been disclosed expressly and sufficiently and the title of the Work and its authorship have been acknowledged in this Work;
- (4) I do not have any actual knowledge nor do I ought reasonably to know that the making of this work constitutes an infringement of any copyright work;
- (5) I hereby assign all and every rights in the copyright to this Work to the University of Malaya ("UM"), who henceforth shall be owner of the copyright in this Work and that any reproduction or use in any form or by any means whatsoever is prohibited without the written consent of UM having been first had and obtained;
- (6) I am fully aware that if in the course of making this Work I have infringed any copyright whether intentionally or otherwise, I may be subject to legal action or any other action as may be determined by UM.



Candidate's Signature

*F.F. Muhammad*

Date

5 March 2012

Subscribed and solemnly declared before,



Witness's Signature

**Dr. Khaulah Sulaiman**  
Jabatan Fizik  
Universiti Malaya  
50603 Kuala Lumpur

Date

5 March 2011

Name: **Dr. Khaulah Sulaiman**

Designation: **Senior Lecturer**

## ABSTRACT

The simple fabrication process involving minimal material usage makes solution-processed organic solar cell (Courses) devices very attractive for harvesting solar energy. However, production of these devices on a commercial scale has been slow due to their relatively low power conversion efficiency and stability problems. It is expected that these obstacles will be surmounted in the future with rigorous studies actively being done in this field of research. Besides, a complete understanding of some basic electrical responses of these OSC devices has not been achieved yet. Consequently, seeking for interesting materials suitable for OSCs application and understanding the materials contribution are of great importance especially when strategies are targeted for the enhancement of OSCs. Tris (8-hydroxyquinolate) metals (Mq<sub>3</sub>) are well known in the fabrication of stable organic light emitting diodes (OLEDs) and also for their unique optoelectronic properties. Very recently, tris (8-hydroxyquinolate) aluminium (Alq<sub>3</sub>) prepared by thermal evaporation has been used as a buffer layer and dopant material to improve the performance of OSCs. However, its employment in solution-processed organic solar cells is still rare. Little attention has been paid on the behaviour of this material when applied in organic solar cells. Therefore, benefiting from the properties of Mq<sub>3</sub> and easy fabrication process of solution-processed organic solar cell, the current thesis is focused on characterizing the OSCs related physical properties of tris (8-hydroxyquinolate) gallium (Gaq<sub>3</sub>) and aluminium (Alq<sub>3</sub>) (as representatives of the Mq<sub>3</sub> materials) and then applying them in solution-processed organic solar cells. The solution-processed OSC devices are based on ternary bulk heterojunction structure (three components blended all together) of dihexylisexithiophen/Mq<sub>3</sub>/methanofullerene (DH6T/Mq<sub>3</sub>/PCBM). The optoelectronics, spectroscopic, electrochemical, structural, morphological, and thermal properties of Mq<sub>3</sub> materials are first investigated before

incorporating them into the photovoltaic active layers of the devices. From the analysis of physical properties of Mq3 materials as well as the assessment on the electrical characteristics of the devices, this work suggests that Mq3 can be a good candidate to be applied in solution-processed OSCs. The photovoltaic and electrical characteristics of the devices demonstrated that the photocurrent, open circuit voltage, and the performance of the devices have improved by approximately six times compared to the devices without Mq3 incorporation. The basic contribution of Mq3 materials for this improvement is believed to originate from the increase in the number of exciton generation and their dissociation into free charge carriers. This can be due to the enlarged area of the donor-acceptors boundaries between each of the DH6T/Mq3 and DH6T/PCBM moieties, thereby broadening the absorption of photons. Next, Mq3 incorporation can result in the stabilization of the mobility of the charge carriers within the DH6T donor and Mq3/PCBM acceptors producing a balanced transportation for the holes and electrons. The results indicated promising approaches for Mq3 materials to be applied in solution-processed OSCs as incorporation of Mq3 into the devices active layers considerably enhanced the overall performance and reproducibility of these devices.

## ABSTRAK

Peranti sel suria organik (Courses) berasaskan larutan sangat menarik bagi menghasilkan tenaga suria kerana melibatkan penggunaan bahan yang minima melalui suatu proses pembuatan yang mudah. Walaubagaimanapun, penghasilan peranti ini pada skala komersial amat perlahan disebabkan kecekapan penukaran kuasa yang rendah secara relatifnya dan masalah kestabilan peranti. Tetapi, apabila kajian penyelidikan yang rapi dalam bidang ini digiatkan, dijangka halangan ini akan dapat diatasi pada masa depan. Pemahaman yang lengkap belum lagi dicapai bagi beberapa aspek asas elektrik dalam peranti OSC ini. Maka, pencarian bahan yang menarik dan sesuai bagi kegunaan OSC dan pemahaman terhadap peranan bahan, merupakan perkara penting terutamanya bagi mengatur strategi untuk meningkatkan prestasi peranti OSC. Logam tris (8-hydroxyquinolate) (Mq3) dikenali ramai dalam penghasilan diod pemancar cahaya organik (OLED) dan juga sifat unik optoelektroniknya. Baru-baru ini, tris (8-hydroxyquinolate) aluminium (Alq3) yang disediakan melalui kaedah pendedapan terma telah digunakan sebagai lapisan penampakan dan bahan pendop bagi meningkatkan prestasi peranti OSC. Namun begitu, penggunaan bahan ini dalam sel suria organik berasaskan larutan masih jarang dijalankan. Hanya sedikit perhatian yang diberikan kepada sifat bahan ini apabila digunakan dalam sel suria organik. Oleh itu, berdasarkan kepada manfaat sifat bahan Mq3 dan proses pembuatan yang mudah untuk menghasilkan sel suria organik berasaskan larutan, tesis ini ditumpukan kepada mencirikan sifat-sifat fizikal berkaitan dengan OSC, yang menggunakan tris (8 hydroxyquinolate) galium (Gaq3) dan Alq3, sebagai wakil daripada bahan Mq3, kemudian menggunakannya dalam pembuatan sel sel suria organik berasaskan larutan. Peranti dibuat berasaskan kepada simpang-hetero pukal ternari dihexylisexithiophen/Mq3/methanofullerene (DH6T/Mq3/PCBM). Sifat optoelektronik,

spektroskopi, elektro-kimia, struktur, morfologi, dan haba merupakan ciri awal yang dikaji sebelum bahan Mq3 digunakan sebagai lapisan aktif dalam peranti fotovoltaik. Hasil kajian ini mencadangkan bahawa Mq3 merupakan suatu bahan yang berpotensi untuk diaplikasikan dalam OSC berasaskan larutan, berdasar kepada analisa ciri fizikal bahan serta taksiran terhadap ciri elektrik peranti tersebut. Ciri fotovoltaik dan ciri elektrik peranti menunjukkan bahawa arus-foto, voltan litar-terbuka, dan prestasi keseluruhan peranti telah meningkat sebanyak kira-kira enam kali berbanding dengan peranti tanpa Mq3. Sumbangan asas bahan Mq3 kepada peningkatan ini, dipercayai berasal daripada peningkatan bilangan eksiton dan pemisahan eksiton menjadi pembawa cas bebas. Ini disebabkan kawasan sempadan penderma-penerima telah dibesarkan antara setiap komponen DH6T/Mq3 dan DH6T/PCBM, yang akhirnya menyebabkan pelebaran bagi serapan foton. Kemudian, penggunaan bahan Mq3 telah menyebabkan angkutan antara lohong dan elektron menjadi seimbang yang berpunca daripada kestabilan mobiliti pembawa cas di antara penderma DH6T dan penerima Mq3/PCBM. Keputusan kajian menunjukkan bahawa bahan Mq3 yang digunakan sebagai bahan lapisan aktif dalam peranti bagi pembuatan OSC berasaskan larutan, mampu memberi peningkatan bagi prestasi keseluruhan serta kebolehasilan-semula peranti ini.

## ACKNOWLEDGEMENTS

First and foremost I would like to thank God, the almighty Allah, for blessing me with sufficient time and health to get my goals. I would like to thank my parents for their patient, all the love, and support they have given me throughout my life. I would also like to acknowledge my supervisor, Dr. Khaulah Sulaiman, for her continuous support and encouragement. The works perused in this thesis would not have been possible without her complete confidence with me.

Special thank to the directorate and staff members of the Ahmed Ismail Foundation–Hawler, Kurdistan Region/Iraq (in association with the Ministry of Higher Education of Kurdistan), for their financial support in the form of Scholarship and their administrative assistance during the whole period of my study.

I also thank the University of Malaya for providing the research grants PS319/2009B and PS343/2010B to support my research works and to participate in the conferences inside and outside Malaysia.

I would like to thank Dr. I. Hernández Campo for his scientific suggestions and language editing in part of my thesis contents. I should also thank Dr. Kamal Aziz Ketuly for providing me with some chemical solvents and Dr. Abdulkader Jaleel Muhammad for establishing an empirical formula used in part of my studies.

More thanks go to all my colleagues at the Low Dimensional Material Research Center (LDMRC), Department of Physics, University of Malaya, for their fruitful and kind help from the beginning time of my research works up until now. Their helps are highly appreciated.

Last but not least, I would like to thank all my friends for their support and inspiration, whoever has helped me even if it was with a nice word or a smile.

*F.F. Muhammad  
March 2012  
Kuala Lumpur*

## RESEARCH PAPERS AND CONFERENCES

### A. Papers Extracted from Thesis Contents

- Muhammad, F. F., Abdul Hapip, A. I., & Sulaiman, K. (2010). Study of optoelectronic energy bands and molecular energy levels of tris (8-hydroxyquinolate) gallium and aluminum organometallic materials from their spectroscopic and electrochemical analysis. *Journal of Organometallic Chemistry*, 695(23), 2526-2531.
- Muhammad, F. F., & Sulaiman, K. (2011). Utilizing a simple and reliable method to investigate the optical functions of small molecular organic films - Alq3 and Gaq3 as examples. *Measurement*, 44(8), 1468-1474.
- Muhammad, F. F., & Sulaiman, K. (2011). Effects of thermal annealing on the optical, spectroscopic, and structural properties of tris (8-hydroxyquinolate) gallium films grown on quartz substrates. *Materials Chemistry and Physics*, 129(3), 1152-1158.
- Muhammad, F. F., & Sulaiman, K. (2011). Photovoltaic performance of organic solar cells based on DH6T/PCBM thin film active layers. *Thin Solid Films*, 519(15), 5230-5233.
- Muhammad, F. F., & Sulaiman, K. (2011). Tuning the optical band gap of DH6T by Alq3 dopant. *Sains Malaysiana*, 40(1), 17-20.
- Muhammad, F. F., & Sulaiman, K. (2011). On the absorption edge energies of the DH6T<sub>(1-x)</sub>:Mq3<sub>(x)</sub> composite systems; (M= Ga, Al). *Materials Science and Engineering: A*, (to be submitted).
- Muhammad, F. F., & Sulaiman, K. (2011). Fabrication and characterization of solution-processed organic solar cells based on ternary bulk heterojunction of DH6T/Mq3/PCBM (M= Ga, Al). *Solar Energy Materials and Solar Cells*, (to be submitted).

### B. Conferences Attended

- National Physics Conference (*PERFIK2009*) - Malacca, Malaysia (Top 20 papers selection).
- Fifth International Conference on Technological Advances of Thin Films and Surface Coatings (*ThinFilms2010*) - Harbin, China (Selection for ISI Journals).
- Third International Conference on Functional Materials and Devices (*ICFMD2010*) - Terengganu, Malaysia (Gold Medal Achievement).



## TABLE OF CONTENTS

TABLE OF CONTENTS .....	VIII
LIST OF FIGURES .....	XII
LIST OF TABLES .....	XVIII
LIST OF SYMBOLS .....	XIX
LIST OF ABBREVIATIONS .....	XXI
<b>CHAPTER 1 MOTIVATION AND THESIS STATEMENT .....</b>	<b>1</b>
1.1 Introduction .....	1
1.2 Motivation .....	2
1.3 Objectives .....	5
1.4 Thesis Outline .....	6
<b>CHAPTER 2 BACKGROUND AND LITERATURE REVIEW .....</b>	<b>9</b>
2.1 Organic Solar Cells .....	9
2.1.1 Historical Background .....	10
2.1.2 Fabrication Techniques .....	13
2.2 Physics and Characterization of OSC Devices .....	15
2.2.1 Photo-absorption and Exciton Generation .....	17
2.2.2 Exciton Diffusion and Dissociation .....	18
2.2.3 Charge Transport and Collection .....	20
2.2.4 Characterization Parameters .....	22
2.3 Approaches to Improve Organic Solar Cells .....	25
2.3.1 Bulk Heterojunction Structure .....	26
2.3.2 Multilayer and Tandem Structures .....	28
2.3.3 Exciton Blocking Layer .....	30
2.3.4 Double Cable Polymer .....	32

2.4 Materials Selection and Energy Bands Alignment .....	33
2.5 Thiophene/Fullerene Based Organic Solar Cells .....	38
2.6 Organic Solar Cells Incorporating Small Molecular Organic Materials.....	43
<b>CHAPTER 3 METHODOLOGY .....</b>	<b>47</b>
3.1 Chemicals and Materials .....	47
3.1.1 Organic Materials and Solvents .....	47
3.1.2 Substrates and Electrodes.....	50
3.1.3 Substrates Patterning and Cleaning.....	51
3.2 Thin Films Coating .....	51
3.2.1 Gaq3 and Alq3 films .....	52
3.2.2 DH6T/Mq3/PCBM Heterostructure Films.....	53
3.3 Characterization Techniques.....	54
3.3.1 Ultraviolet-Visible-Near Infrared (UV-Vis-NIR) Spectrophotometer.....	54
3.3.2 Photoluminescence (PL) Spectroscopy.....	57
3.3.3 Fourier Transform Infrared (FTIR) Spectrophotometer .....	59
3.3.4 X-Ray Diffraction (XRD) Technique .....	63
3.3.5 Cyclic Voltammetry (CV).....	67
3.3.6 Differential Scanning Calorimetry (DSC) .....	70
3.3.7 Scanning Electron Microscopy .....	74
3.3.8 Surface Profilometer .....	76
3.4 Devices Fabrication and Measurement .....	78
3.4.1 Bilayer and Bulk Heterostructures .....	78
3.4.2 Ternary Bulk Heterojunction .....	80
3.4.3 Photovoltaic Measurements .....	81

## **CHAPTER 4 CHARACTERIZATION OF TRIS (8-HYDROXYQUINOLINATE)**

<b>METALS</b> .....	84
4.1 Preliminary .....	84
4.2 Transmission Spectra and Thickness Measurement .....	85
4.3 Optoelectronics and Spectroscopic Studies .....	88
4.3.1 Absorption Bands Assignment.....	88
4.3.2 Energy Gap Determination .....	91
4.3.3 Refractive Index and Dielectric Parameters.....	94
4.3.4 Photoluminescence Behavior .....	100
4.4 Electrochemical Analysis.....	101
4.4.1 Molecular Energy Levels .....	102
4.4.2 Energy Bands Diagram .....	104
4.5 Structural and Morphological Investigations .....	105
4.6 Thermal Properties .....	108
4.6.1 Glass Transition Temperature .....	108
4.6.2 Crystalline and Melting Temperatures.....	111
4.7 Effects of Thermal Annealing on the Optical, Spectroscopic, and Structural Properties .....	112
4.8 Summary .....	123
<b>CHAPTER 5 DEVICES INCORPORATING TRIS (8-HYDROXYQUINOLINATE)</b>	
<b>METALS</b> .....	126
5.1 Preliminary .....	126
5.2 DH6T/Mq3/PCBM Heterostructure Films.....	128
5.2.1 Photoabsorption Response .....	128
5.2.2 Photoluminescence Behavior .....	135
5.3 Devices Based on DH6T/PCBM Bilayer and Bulk Heterostructure .....	137
5.4 Devices Based on DH6T/Mq3/PCBM Ternary Bulk Heterojunction.....	142

5.4.1 Current-Voltage and Power-Voltage Characteristics.....	143
5.4.2 Series and Parallel Resistances .....	147
5.4.3 Equivalent Circuit and Charge Transport Properties .....	150
5.5 Summary .....	154
<b>CHAPTER 6 CONCLUSIONS AND FUTURE WORKS .....</b>	<b>155</b>
6.1 Conclusions .....	155
6.2 Future Works.....	159

## LIST OF FIGURES

Figure 1.1: Human development index (HDI) versus per capita kWh electricity use. ....	2
Figure 1.2: World photovoltaic electricity production capacity from 1990 to 2008. ....	3
Figure 2.1: Structure of organic based solar cell devices.....	10
Figure 2.2: Photographic picture of some techniques used for coating and printing active layers of OSC; (a) spin coating, (b) doctor balding, (c) screen printing, (d) ink-jet printing, (e) pad printing and (f) role-to-role technique.....	14
Figure 2.3: An equivalent circuit which models OSC devices. ....	16
Figure 2.4: Photo-absorption and exciton generation processes in OSC devices.....	18
Figure 2.5: Schematic diagram of exciton diffusion and dissociation processes in OSC devices (Black circle represents hole, while red circle represents electron).....	20
Figure 2.6: Charge transport and collection process in OSC devices.....	21
Figure 2.7: <i>J-V</i> characteristic of OSC devices. ....	22
Figure 2.8: shows (a) solar irradiance spectrum above atmosphere and at surface, and (b) air masses at different sun zenith angle.....	23
Figure 2.9: Bulk heterojunction structure between ITO and Al electrodes. ....	27
Figure 2.10: SEM side views of MDMO-PPV:PCBM blend films with various ratios of MDMO-PPV to PCBM, (a) 1:2, (b) 1:4 and (c) 1:6, on top of PEDOT: PSS coated ITO glass.....	28
Figure 2.11: The structure of (a) multilayer organic p-i-n solar cells and (b) organic tandem solar cells.....	30
Figure 2.12: OSC device incorporating exciton blocking layer of Alq3 between the cathode electrode and acceptor material. ....	31
Figure 2.13: OSC device incorporating exciton blocking layer of PEDOT:PSS between the anode electrode and acceptor material. ....	32

Figure 2.14: Shows (a) schematic representation of a realistic double-cable polymer where interchain interactions are considered, and (b) self-assembled layered structure of di-block copolymers.....	33
Figure 2.15: The correct HOMO and LUMO energy band alignment of DH6T, Gaq3 and PCBM, from left to right, respectively for the OSCs application. ....	37
Figure 2.16: The carbon-carbon double bond conjugation and its <i>p</i> -electron clouds. ....	38
Figure 3.1: The chemical structure of (a) Mq3 (M = Al, Ga, and q = 8-hydroxyquinolate), (b) DH6T, (c) PCBM, and (d) PEDOT:PSS.....	49
Figure 3.2: (a) The chemical structure of Mq3, (b) the schematic diagram of the deposited Mq3 films on the transparent quartz slides, and (c) the schematic diagram of the thermal evaporator set-up.....	53
Figure 3.3: The spin coating machine that is used to deposit active layers for the characterization and devices fabrication purposes. ....	54
Figure 3.4: Photograph of Jasco V-570 UV-Vis-NIR spectrophotometer.....	55
Figure 3.5: Electronic energy levels and transitions involving in UV-Vis absorption. ...	56
Figure 3.6: Operating principle of the UV-Vis spectrophotometers.....	57
Figure 3.7: Photograph of LS50B Perkin Elmer luminescence spectrometer. ....	58
Figure 3.8: (a) Luminescence process, and (b) operating principle of the PL spectrometers.....	59
Figure 3.9: Photograph of Nicolet IS10-Thermo Scientific FTIR spectrophotometer. ...	60
Figure 3.10: The approximate regions where stretching vibrations occur for various common types of bonds. ....	61
Figure 3.11: The approximate regions where stretching vibrations occur for various common types of bonds. ....	63
Figure 3.12: Photograph of the used X-ray diffractometer machine (Bruker AXS).....	64
Figure 3.13: Diffraction of X-rays by planes of atoms (A–A' and B–B').....	66

Figure 3.14: Schematic diagram of an X-ray diffractometer. ....	67
Figure 3.15: The potentiostat and MCA microcell used for CV analysis experiment. ....	68
Figure 3.16: (a) Set up of the CV cell electrodes connection, and (b) the current-voltage curve of a standard CV test. ....	70
Figure 3.17: TA Differential Scanning Calorimetry instrument, DSC Q200. ....	71
Figure 3.18: TA Differential Scanning Calorimetry instrument, DSC Q200. ....	72
Figure 3.19: The general feature of DSC curve. ....	73
Figure 3.20: Field emission scanning electronic microscope (FESEM, Quanta 200F). ..	74
Figure 3.21: Principal features of a SEM. ....	75
Figure 3.22: KLA Tensor P-6 surface profilometer instrument. ....	77
Figure 3.23: (a) A texture profile image recorded by surface profilometers, and (b) the process by which a surface is scanned under noncontact tip condition. ....	78
Figure 3.24: Schematic views of the devices geometry; (a) ITO/DH6T/PCBM/Al with donor-acceptor bilayer structure, (b) ITO/PEDOT:PSS/DH6T/PCBM/Al with donor-acceptor bilayer structure, (c) ITO/PEDOT:PSS/DH6T:PCBM/Al with blended donor-acceptor structure and (d) the energy bands of their component materials. ....	80
Figure 3.25: Schematic views of devices with (a) DH6T:Mq3:PCBM ternary bulk heterojunction, and (b) DH6T:PCBM bulk heterojunction active layers. ....	81
Figure 3.26: An Oriel solar simulator- model 67005. ....	82
Figure 3.27: Shows (a) a Keithley 236 source measurement instrument, and (b) a solar cell device connected to its terminal leads for the <i>I-V</i> measurement. ....	83
Figure 4.1: Transmittance spectra of Gaq3 and Alq3 films. ....	86
Figure 4.2: Transmission spectra of the films in the high transparency range that shows the generated interference fringes. ....	87
Figure 4.3: Absorption spectra of Gaq3 and Alq3 films showing relatively broad electronic absorption peak. ....	90

Figure 4.4: FTIR spectra of the Gaq3 and Alq3 films at their finger print zone. ....	91
Figure 4.5: Plot of $d \ln(\alpha h\nu) / dh\nu$ versus $E$ for Gaq3 and Alq3 films (the inset figure, $\ln(\alpha h\nu)$ vs. $\ln(h\nu - E_g)$ plotted to determine the value of $n$ . ....	93
Figure 4.6: Plot of $(\alpha h\nu)^2$ versus photon energy $E$ for Gaq3 and Alq3 films. ....	93
Figure 4.7: Refractive index dispersion for Gaq3 and Alq3 films. ....	95
Figure 4.8: Absorption coefficient spectra of the studied organic films, Gaq3 and Alq3. ....	97
Figure 4.9: Extinction coefficient spectra for Gaq3 and Alq3 films. ....	97
Figure 4.10: Real part dielectric dispersion for Gaq3 and Alq3 films. ....	99
Figure 4.11: Imaginary part dielectric spectra for Gaq3 and Alq3 films. ....	99
Figure 4.12: Dielectric loss tangent spectra for Gaq3 and Alq3 films. ....	100
Figure 4.13: Normalized PL emission of Gaq3 and Alq3 films. ....	101
Figure 4.14: Cyclic voltammograms of Gaq3 and Alq3 in $\text{CH}_2\text{Cl}_2$ solution. ....	103
Figure 4.15: Band gap and molecular energy levels diagram for Gaq3 and Alq3. ....	105
Figure 4.16: The XRD diffraction patterns for Gaq3 and Alq3 in powder and film forms. ....	106
Figure 4.17: The FESEM surface images of (a) Gaq3, and (b) Alq3 films. ....	107
Figure 4.18: DSC thermograms for (a) Alq3, and (b) Gaq3 compounds with acetone as plasticizer. ....	110
Figure 4.19: Absorption spectra of the as-deposited and annealed films from 85 °C to 255 °C under nitrogen gas for 10 min. ....	114
Figure 4.20: Plot of $(\alpha E)^2$ versus $h\nu$ for the as-deposited and annealed films from 85 °C to 255 °C under nitrogen gas for 10 min. ....	115
Figure 4.21: PL spectra of the as-deposited and annealed films from 85 °C to 255 °C under nitrogen gas for 10 min. ....	117



Figure 4.22: Variation in the optical energy gap and peak PL intensity for the Gaq3 films annealed at different temperatures under nitrogen gas for 10 min. ....	118
Figure 4.23: Variation in the peak PL position and its full wave at half maximum (FWHM) for the Gaq3 films annealed at different temperatures under nitrogen gas for 10 min. ....	119
Figure 4.24: FTIR spectra of the powder, as-deposited and annealed Gaq3 films at various annealing temperatures under nitrogen gas for 10 min. ....	121
Figure 4.25: XRD diffraction patterns for the Gaq3 powder, as-deposited and annealed films (annealed from 85 °C to 255 °C under nitrogen gas for 10 min). ....	123
Figure 5.1: Absorption spectra of DH6T/Gaq3 blends: Influence of Gaq3 contents in DH6T solution.....	129
Figure 5.2: The DH6T:Gaq3 (1:X ratio) blend solutions prepared in the vials. ....	130
Figure 5.3: Plots of $(\alpha E)^2$ against photon energy $E$ for the films of pure DH6T and DH6T:Alq3 blends.....	131
Figure 5.4: Plot of DH6T:Alq3 absorption edge energy versus molar concentration of Alq3.....	133
Figure 5.5: Normalized absorbance of DH6T, PCBM and DH6T/PCBM blend films with and without incorporating Mq3.....	135
Figure 5.6: Photoluminescence spectra of DH6T, DH6T/Alq3/PCBM and DH6T/Gaq3/PCBM films excited at 360 nm.....	137
Figure 5.7: The $J-V$ characteristics of the organic solar cells with device A- DH6T/PCBM (BL), device B- PEDOT:PSS/DH6T/PCBM (BL) and device C- PEDOT:PSS/DH6T:PCBM (1:1 BHJ).....	139
Figure 5.8: The $P-V$ characteristics of the organic solar cells composed of A- DH6T/PCBM (BL), B- PEDOT:PSS/DH6T/PCBM (BL) and C- PEDOT:PSS/DH6T:PCBM (1:1 BHJ) active layers. ....	141

Figure 5.9: Device structures of (a) DH6T:Mq3:PCBM ternary bulk heterojunction, and (b) DH6T:PCBM bulk heterojunction devices. ....	142
Figure 5.10: The $J-V$ characteristics of the bulk heterojunction devices with and without incorporated Mq3.....	144
Figure 5.11: The HOMO and LUMO energy levels alignment between the DH6T/Ga <sub>q</sub> 3/PCBM (a) and DH6T/Al <sub>q</sub> 3/PCBM (b) ternary bulk heterojunction active layers. ....	145
Figure 5.12: The $P-V$ characteristics of the bulk heterojunction devices with and without incorporated Mq3.....	147
Figure 5.13: The $J-V$ characteristics of the devices with and without incorporated Mq3, illustrating the regions where $R_s$ and $R_{sh}$ of the devices can be extracted.....	148
Figure 5.14: The influence of Mq3 in the D3HT:PCBM-based devices on $J-V$ characteristics in the dark and upon light illumination.....	149
Figure 5.15: The light and dark semi log $J-V$ characteristics of a representative device under investigation.....	151
Figure 5.16: The double logarithmic plot of $J-V$ characteristics for the devices with and without incorporated Mq3 in the dark condition.....	152
Figure 5.17: The semi-log $J-V$ characteristic of a representative device in the dark condition; inset of the Figure depicts the equivalent circuit of OSCs.....	153

## LIST OF TABLES

Table 2.1: Some notable events in the history of organic solar cells.....	12
Table 2.2: The nomenclature, molecular energy levels, and structure of some representative organic donor and acceptor materials.....	35
Table 3.1: The organic materials, their respective solvent(s), and concentration of the solutions prepared for various studies.....	50
Table 4.1: Thickness values of the organic thin films, Gaq3 and Alq3, analyzed and calculated from their transmittance spectra.....	88
Table 4.2: The measured optical energy gap, $E_g$ for the organic films, Gaq3 and Alq3.	94
Table 4.3: Estimated molecular energy levels, and optoelectronic energy gap ( $E_g$ ) for Gaq3 and Alq3 obtained from the electrochemical analysis and spectroscopic data. ..	104
Table 4.4: Tabulates the variation in peak PL intensity, peak PL position, FWHM, Stokes shift, and optical energy gap of Gaq3 film annealed at different temperatures under nitrogen gas atmosphere for 10 min.....	117
Table 4.5: IR absorption bands assignment for Gaq3.....	121
Table 5.1: The average value of the obtained photovoltaic parameters for the studied organic solar cell devices. ....	138
Table 5.2: The photovoltaic and physical parameters of the solar cell devices obtained with and without incorporated Mq3.....	150

## LIST OF SYMBOLS

$I_{sc}$	Short circuit current
$\eta_{diff}$	Exciton diffusion efficiency
$\eta_{tc}$	Hole-electron separation efficiency
$\eta_{tr}$	Carrier transport efficiency
$\eta_{cc}$	Charge collection efficiency
$n_{\infty}$	Refractive indices at infinite wavelength
$\hat{n}$	Complex refractive index
$\hat{\epsilon}$	Complex dielectric constant
$\epsilon_r$	Real dielectric constant
$\epsilon_i$	Imaginary dielectric constant
$\tan \delta$	Dissipation factor
$\alpha$	Absorption coefficient
$\Phi_s$	Volume fraction of solvent
$T_{gs}$	Glass transition temperature of solvent
$T_{ms}$	Melting temperature of solvent
$\lambda$	Wavelength
$\theta$	Angle of diffraction
$\Delta\lambda_{1/2}$	Full width at half maximum (FWHM)
$A$	Absorbance
$c$	Velocity of light
$d$	Interplanar spacing
$D-A$	Donor-Acceptor
$E$	Photon energy
$e$	Electronic charge unit
$E_{abs}$	Absorption edge
$E_g$	Band gap energy
$E_{red}$	Reduction potential
$FF$	Fill factor
$h$	Planck's constant
$h$	Planck's constant

$I_{max}$	Current at maximum power
$J$	Current density
$J_L$	Photo-generated current density
$J_o$	Saturation current density
$J_{sc}$	Short circuit current density
$k$	Extinction coefficient
$L$	Mean free path of charge carriers
$n$	Refractive index
$N_A$	Acceptor density
$N_C$	Densities of states in the conduction band
$N_V$	Densities of states in the valence band
$P_{in}$	Input power, incident photon energy power
$P_m, P_{max}$	Maximum power
$R_s$	Series resistance
$R_{sh}, R_p$	Shunt resistance, parallel resistance (having same physical meaning)
$S$	Substrate refractive index
$T$	Transmittance
$T_c$	Crystalline temperature
$T_g$	Glass transition temperature
$T_m$	Melting temperature
$T_{max}$	Transmission maxima
$T_{min}$	Transmission minima
$V_f$	Diode potential barrier
$V_{max}$	Voltage at maximum power
$V_{oc}$	Open circuit voltage
$\eta$	Power conversion efficiency
$\mu$	Charge carrier mobility
$\nu$	Frequency

## LIST OF ABBREVIATIONS

Al	Aluminum
Alq3	tris (8-hydroxyquinolate) aluminum
AM	Air mass
Au	Gold
BCP	Bathocuproine
BHJ	Bulk heterojunction
BL	Bilayer
C <sub>60</sub>	Buckminsterfullerene
Ca	Calcium
CB	Conduction band
CLB	Chlorobenzene
CNTs	carbon nanotubes
CS <sub>2</sub>	Carbon disulphide
c-Si	crystalline silicon
CuPc	Copper phthalocyanine
CV	Cyclic voltammetry
DH6T	dihexyl-sexithiophene
DIW	distilled water
DMSO	Dimethyl sulphoxide
DSC	Differential scanning calorimetry
<i>EA</i>	Electron affinity
EBL	Exciton blocking layer
EM	Electron microscopy
<i>EQE</i>	External quantum efficiency
ETL	Electron transport layer
FESEM	Field emission scanning electron microscopy
FTIR	Fourier transform infrared
FWHM	Full width at half maximum
GaAs	gallium arsenide
Gaq3	tris (8-hydroxyquinolate) gallium
GNDU	Ground unit
HCl	hydrochloric acid
HDI	Human Development Index

HOMO	higher occupied molecular orbital
<i>IP</i>	Ionization potential
<i>IQE</i>	Internal quantum efficiency
ITO	Indium-tin-oxide
kWh	kilowatt-hours
LiF	Lithium fluoride
LM	Light microscopy
LUMO	lower unoccupied molecular orbital
MEH-PPV	poly(2-methoxy-5(2'-ethyl) hexoxy-phenylenevinylene)
Mg	Magnesium
MIM	metal-insulator-metal
MPP	maximum power point
Mq3	tris (8-hydroxyquinolate) metals
OFET	Organic field effect transistor
OLED	organic light emitting diode
OLEDs	Organic light emitting diodes
P3HT	poly-3-hexylthiophene
PCBM	6,6-phenyl C <sub>61</sub> -butyric acid methyl ester
PCPDTBT	poly[2,6-(4,4-bis-(2-ethylhexyl)-4H-cyclopenta[2,1-b;3,4-b']-dithiophen)-alt-4,7-(2,1,3-benzothiadiazole)]
PDTSTPD	thieno[3,4-c]pyrrole-4,6-dione and Dithieno[3,2- <i>b</i> :20,30- <i>d</i> ]silole
PEDOT-PSS	poly(3,4-ethylenedioxythiophene):poly(4-styrenesulfonic) acid
PL	Photoluminescence
PPV	Poly( <i>p</i> -phenylenevinylene)
PTB4	fluorinated thieno[3,4- <i>b</i> ] thiophene and benzodithiophene units
PTCBI	3,4,9,10-perylene tetracarboxylic-bisbenzimidazole
PV	photovoltaic
RES	Renewable Energy Sources
RS	Rayleigh scattering
SCE	Saturated calomel electrode
SCLC	Space charge limited current
SEM	Scanning electron microscopy
SHE	Standard hydrogen electrode (platinum)
SMU	Source measure unit
STC	Standard test condition

TBJH	Ternary bulk heterojunction
TCAQ	tetracyanoanthraquino-dimethane
TFSCLC	Trap-filling space charge limited current
UV-Vis-NIR	Ultraviolet- Visible- Near Infrared
VB	Valence band
XRD	X-ray diffraction
ZnPc	Zincphthalocyanine
3D	Three dimensions
4T	Quarter-thiophene oligomer
6T	Sexi-thiophene oligomer